EUKARYOTIC CELL, July 2005, p. 1253–1263 Vol. 4, No. 7
1535-9778/05/$08.00+0 doi:10.1128/EC.4.7.1253–1263.2005

Centrin Scaffold in *Chlamydomonas reinhardtii* Revealed by Immunoelectron Microscopy

Stefan Geimer* and Michael Melkonian

Botanisches Institut, Universität zu Köln, D-50931 Köln, Germany

Received 7 March 2005/Accepted 10 May 2005

In the flagellate green alga *Chlamydomonas reinhardtii* the Ca^{2+}-binding EF-hand protein centrin is encoded by a single-copy gene. Previous studies have localized the protein to four distinct structures in the flagellar apparatus: the nucleus-basal body connector, the distal connecting fiber, the flagellar transitional region, and the axoneme. To explain the disjunctive distribution of centrin, the interaction of centrin with as yet unknown specific centrin-binding proteins has been implied. Here, we demonstrate using serial section postembedding immunoelectron microscopy of isolated cytoskeletons that centrin is located in additional structures (transitional fibers and basal body lumen) and that the centrin-containing structures of the basal apparatus are likely part of a continuous filamentous scaffold that extends from the nucleus to the flagellar bases. In addition, we show that centrin is located in the distal lumen of the basal body in a rotationally asymmetric structure, the V-shaped filament system. This novel centrin-containing structure has also been detected near the distal end of the probasal bodies. Taken together, these results suggest a role for a rotationally asymmetric centrin "seed" in the growth and development of the centrin scaffold following replication of the basal apparatus.

Centrin (also known as caltractin) is a member of the highly conserved superfamily of calcium-binding EF-hand proteins and occurs in all eukaryotic cells, being mostly associated with centrosomes (58, 64). It was first discovered in flagellate green algae, where it is located in the basal apparatus (the part of the cytoskeleton anchoring the flagella) and involved in the contraction of calcium-sensitive filaments (42, 60) which, in general, play an important role in the dynamic behavior of centrosomes by controlling the position and orientation of centrosomal structures (58, 64). Analysis of centrin mutants and RNA interference strains deficient in centrin in the green algal model system *Chlamydomonas reinhardtii* suggested that centrin is essential for basal body duplication and segregation during cell division (28, 39, 73), functions also deduced for centrin homologues in vertebrates (46, 62) and yeast spp. (3, 50, 69). More recently, novel centrin functions have been discovered such as involvement in recombinational DNA repair through modulation of the nucleotide excision repair pathway in humans and plants (2, 47), a role in the nuclear mRNA export machinery in yeast (11), regulation of calcium-dependent ciliary activities in ciliates (14, 15), and signal transduction in vertebrate photoreceptors (53). How centrin exerts these different functions at the molecular level is, however, still unknown although considerable progress has recently been made through in vitro studies of centrin and its interaction with target peptides (8, 19, 20, 40, 75).

In some organisms, the functional diversity of centrin may be related to the presence of different centrin isotypes, e.g., four centrin proteins (centrin1p to centrin4p), which are differentially expressed in different tissues and cell types, have been identified so far in mammals (10, 12, 29, 34, 35, 45). In the ciliate *Paramecium*, three centrin genes have been characterized to date (38) and in another ciliate (*Paraurostyla*) evidence has been presented for differential localization of two centrin isotypes (36).

In *Chlamydomonas reinhardtii* and other flagellate green algae, in which centrin localization and function have been well studied for over 20 years, only a single centrin gene is present (6, 21). The protein, however, has been found at six distinct locations within the cytoskeleton: the nucleus-basal body connector (NBBC), the distal connecting fiber, the flagellar transitional region, the basal body lumen, the axoneme, and the probasal bodies (22, 31, 42, 60, 63, 67, 77). It has thus been suggested that the specificity of centrin localization in green algae may perhaps be provided by different centrin-binding proteins (27). Centrin-binding proteins have been difficult to identify and are mostly known only from yeast (i.e., Kar1p, Kic1p, Mps3p, and Sfi1p) (7, 23, 25, 70, 72). One of these proteins, Sfi1p, however, is also present in mammals (25) and is apparently homologous to a centrin-binding protein (CBP1.1) previously identified in the flagellate green alga *Spermatozopsis similis* (71). This protein contains multiple internal repeats, with each repeat binding one centrin molecule. It is likely that Sfi1p forms filaments on which centrin molecules are arranged like a string of pearls, providing an elegant mechanism for filament contraction by supercoiling (25, 57).

Here we show using serial section postembedding immunoelectron microscopy of isolated cytoskeletons of *Chlamydomonas reinhardtii* that the previously identified distinct localizations of centrin are part of a continuous filamentous scaffold that extends from the nucleus to the base of the axonemes. We describe the intricate association of the centrin scaffold with the basal bodies and demonstrate rotational asymmetry of centrin distribution in the distal lumen of the basal bodies. The distal ends of basal bodies are thought to represent a center of rotational asymmetry in the cytoskeleton of flagellate/ciliate cells (13).

* Corresponding author. Mailing address: Universität Bayreuth, Biologie/Elektronenmikroskopie NW I / B 1, Universitätsstr. 30, D-95447 Bayreuth, Germany. Phone: 49 921 55 2164. Fax: 49 921 55 4301. E-mail: stefan.geimer@uni-bayreuth.de.

MATERIALS AND METHODS

Strains and culture conditions. *Chlamydomonas reinhardtii* cw15$^+$ Dangeard (SAG 83.81) (65) was cultured in aerated 10-liter flasks (approximately 1 liter · min^{-1}) at 15°C with a light-dark cycle of 14:10 h and a photon flux density of 20 $\mu E \cdot m^{-2} \cdot s^{-1}$ (Osram 40W/25 universal white) in WarisH culture medium (41).

Postembedding immunogold electron microscopy. Cytoskeletons of *Chlamydomonas reinhardtii* cw15$^+$ were isolated as previously described (77) and fixed in MT buffer (30 mM HEPES, 5 mM Na-EGTA, 15 mM KCl, pH 7.0) containing 2% paraformaldehyde and 0.25% glutaraldehyde for 40 min at 15°C. After two brief washes with MT buffer, the cytoskeletons were dehydrated to 100% ethanol (30% and 50% ethanol on ice; then 70%, 95%, and 100% ethanol at −20°C, 15 min each). Infiltration of the sample with LR Gold resin (Plano, Marburg, Germany) was performed at −20°C according to the following scheme: LR Gold/ethanol (1:3) for 2 h, LR Gold/ethanol (3:1) for 2 h, LR Gold with 0.4% benzyl for 24 h. Polymerization was performed under fluorescent light for 24 h at −20°C. Control cytoskeletons were fixed and embedded for standard electron microscopy as previously described (13).

Ultrathin sections (60 to 80 nm) were cut with a diamond knife (Diatome, Biel, Switzerland) on an MT-6000 microtome (RMC, Tucson, AZ) and collected on pioloform-coated nickel grids. The sections were blocked for 1 to 3 h at room temperature with blocking buffer (2% bovine serum albumin, 0.1% fish gelatin, and 0.05% Tween 20 in phosphate-buffered saline [PBS]; pH 7.4) and incubated in anti-centrin immunoglobulin G (IgG) immune serum (1:100 in blocking buffer) (17) overnight at 4°C. Purified IgG preimmune serum (same dilutions as the immune serum) was used as control. Grids were washed three to five times with PBS for 10 min each and incubated for 1 to 3 h with 10- or 15-nm gold particles conjugated to goat anti-rabbit IgGs (British BioCell, Cardiff, United Kingdom) diluted 1:30 in blocking buffer. Grids were washed three to five times with PBS for 10 min each, fixed for 8 min in 1% glutaraldehyde in PBS, and washed twice for 8 min each in Milli-Q water. Specimens were stained with lead citrate and uranyl acetate (55) and photographed on a Philips CM 10 transmission electron microscope using Scientia EM film (Agfa, Leverkusen, Germany). In cross sectioned basal bodies or axonemes the view is from the distal to the proximal end.

RESULTS

The ultrastructure of the *Chlamydomonas reinhardtii* basal apparatus has been recently reevaluated in detail using dual-axis electron tomography of whole cells (48) and serial thin-section electron microscopy of isolated cytoskeletons (13), and the reader is referred to these publications for details of terminology and structural components of the basal apparatus. In this communication we used serial section postembedding immunogold electron microscopy on isolated cytoskeletons of *C. reinhardtii* to localize centrin in the basal apparatus. The results are illustrated in Fig. 1 to 4 and summarized in the schematic presentation of Fig. 5. In addition, we performed extensive statistical analyses of the distribution of gold particles (coated with secondary antibody) over individual basal apparatus components by comparing sections exposed to immune versus preimmune centrin IgGs (Table 1).

In general, postembedding immunogold electron microscopy has the advantage over the preembedding technique that antigens inaccessible to gold particles (i.e., those located within other structural components such as basal bodies) become exposed in sections. Progress in preserving fine details of non-osmicated cellular structures and the establishment of a detailed structural map of all basal apparatus components of *C. reinhardtii* (13) facilitate assignment of gold particles (within the resolution determined by the size of the gold-antibody complexes) to specific structures, thus eliminating one of the traditional problems of the postembedding technique. Our preimmune controls revealed no or extremely few gold particles (Fig. 1, panels 11 and 18; Table 1), thus increasing the specificity and sensitivity of the labeling. As a critical test of this approach we investigated centrin labeling over axonemal cross sections (Table 1; Fig. 1, panels 1 to 3). About 42% of the axonemes were labeled (with an average labeling density of 1.8 gold particles/axonemal cross section; $n = 536$). In preimmune controls, only 6% of the axonemes were labeled ($n = 334$). Next, we analyzed where this labeling occurred, probing 117 labeled, randomly chosen axonemal cross sections (displaying a total of 194 gold particles). We found that 96 (82%) of the cross sections showed labeling over the outer doublet microtubules and 21 (18%) were labeled in other axonemal areas (mostly over the central pair microtubules). Thus, centrin labeling in the axoneme was nonrandom and mostly confined to the outer doublet microtubules (often associated with the A tubule; Fig. 1, panels 1 to 3). No centrin labeling of the outer doublet microtubules was observed in the transitional region (the most proximal region) of the axoneme. Centrin is known as a light chain associated with one type of inner dynein arm (33, 52) (see Discussion), which is not present in this region (18).

In contrast to the relatively weak anticentrin labeling in the axoneme, the star-like pattern and ring-like hub of the flagellar transitional region (well-known locations of centrin) were strongly labeled by gold particles (Fig. 1, panels 4 to 10 and 12). The statistical analysis revealed that 85% of the cross sections analyzed ($n = 39$) were labeled, with an average labeling density of 9.9 gold particles/transitional region (Table 1). In the preimmune control, only 3% of the transitional regions were labeled and the labeling density was low (on average 1 gold particle/transitional region). Because of the high labeling density, the distribution of label over the transitional region was not analyzed statistically. However, we noticed that the labeling was more intense over the central ring-like hub compared to the peripheral star-like pattern (Fig. 1, panels 4 to 10). In longitudinal sections of the transitional region both the distal and proximal stellate structures were labeled (Fig. 1, panels 7 to 10). Interestingly, in such sections we often encountered string-like centrin labeling extending centrally from the distal end of the distal stellate structure through the proximal stellate structure to the distal end of the basal body (Fig. 1, panels 7 to 9). The latter part of the string-like labeling corresponds to a previously identified fine filament that extends from the proximal stellate structure to a V-shaped filament system at the distal end of the basal body (13) (compare also Fig. 1, panels 8 and 9 with panels 10 and 11). The distal end of the basal body has been previously shown to contain two different filament systems, both positioned in a rotationally asymmetric manner, namely, the "acorn" and the V-shaped filament system (13) (Fig. 4, panels 37 and 38, and 5, panels 41 and 42 [schematic presentations]). The acorn, a fiber outlining the shape of an acorn in cross sections through basal bodies, is attached to triplets 7, 8, 9, 1, and 2 and is thus located in the part of the basal body facing the opposite basal body (Fig. 5, panels 39, 41, and 44). In longitudinal sections through basal bodies the V-shaped filament system is obliquely oriented (Fig. 1, panels 10, 11, and 20, and 5, panel 39). Its upper (distal) part is located at nearly the same level but opposite to the acorn and consists mainly of two 8-nm-thick filaments, which extend from microtubule triplets/doublets 4 and 5 (mostly the A tubules) into the center of the basal body lumen, where they converge, hence their V-shape in cross sections through basal bodies (Fig. 4,

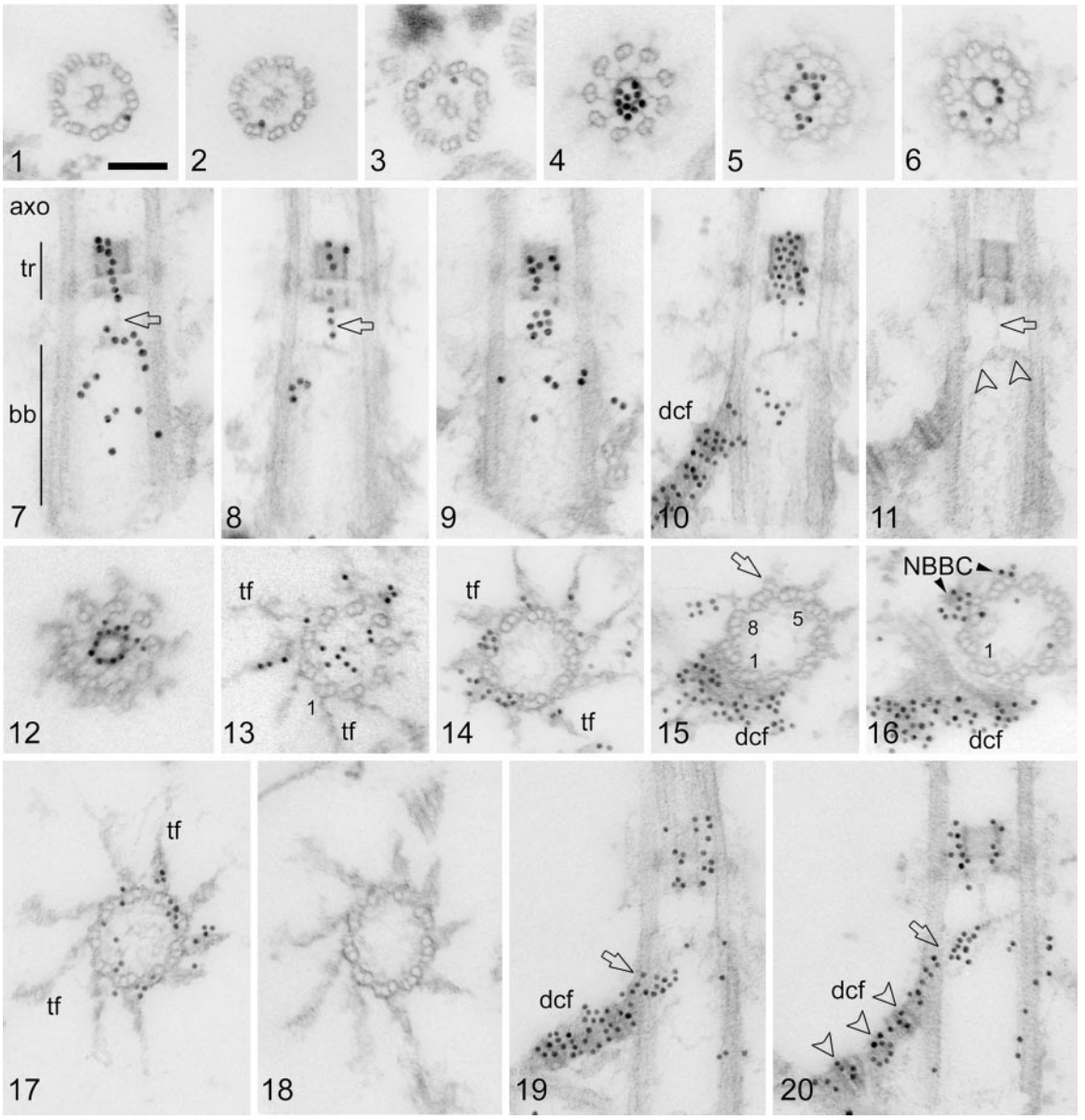

FIG. 1. Postembedding immunogold labeling of centrin in isolated cytoskeletons of *Chlamydomonas reinhardtii*. Shown are 15-nm gold particles (1 to 9), 10-nm gold particles (10, 12 to 17, 19, and 20), and preimmune controls (11 and 18). Scale bar: 0.1 μm. (1 to 3) Random cross sections through axonemes showing gold particles associated primarily with the A tubules of the outer axonemal doublets. (4 to 6) Random cross sections through the flagellar transitional region with dense centrin labeling, mostly over the central ring-like hub. (7 to 10) Random longitudinal sections through the axoneme (7; axo), transitional region (7; tr), and basal body (7; bb). Centrin labeling is found in both the distal and the proximal stellate structures of the transitional region and in a string-like arrangement that extends in the center of the transitional region from the distal stellate structure through the proximal stellate structure towards the distal lumen of the basal body (7 and 8; arrows). Centrin labeling is also seen in the basal body lumen (7, 9, and 10) and in the distal connecting fiber (10; dcf). (11 [preimmune control]) A fine filament (arrow) connects the proximal stellate structure with the V-shaped filament system (arrowheads); both structures contain centrin (see panels 7 to 9 and 20). (12 to 16) Serial cross sections through a transitional region (12) and basal body (13 to 16) showing centrin labeling in the central hub of the stellate structure (12) and in the V-shaped filament system (13 [the V filaments, being delicate and on the surface of the section, are not themselves readily visible in this oblique cross section; the V-shaped filament system is decorated by gold particles across the basal body lumen]), in the transitional fibers (13 and 14; tf), in the distal connecting fiber (15 and 16; dcf), and in the NBBC (16). Basal body triplets 1, 8, and 5 are numbered (13, 15, and 16). The arrow in panel 15 depicts the proximal end of a transitional fiber, and the next section in the series reveals centrin labeling on the same triplet (no. 7) at the attachment site of the NBBC. (17) Cross section through the distal part of a basal body in the region of the transitional fibers (tf) showing centrin labeling over the proximal parts of several transitional fibers as well as in the basal body lumen and the doublet/triplet interlinkers. A fine meshwork of filaments extends throughout the basal body lumen (17). (19 and 20) Two random longitudinal sections through basal bodies depicting strong centrin labeling over the distal connecting fiber (dcf). Centrin labeling was more prominent over the electron-dense striations of the distal connecting fiber (arrowheads in panel 20; see also panel 10). Centrin labeling is continuous between the distal connecting fiber and the V-shaped filament system (19 and 20; arrows).

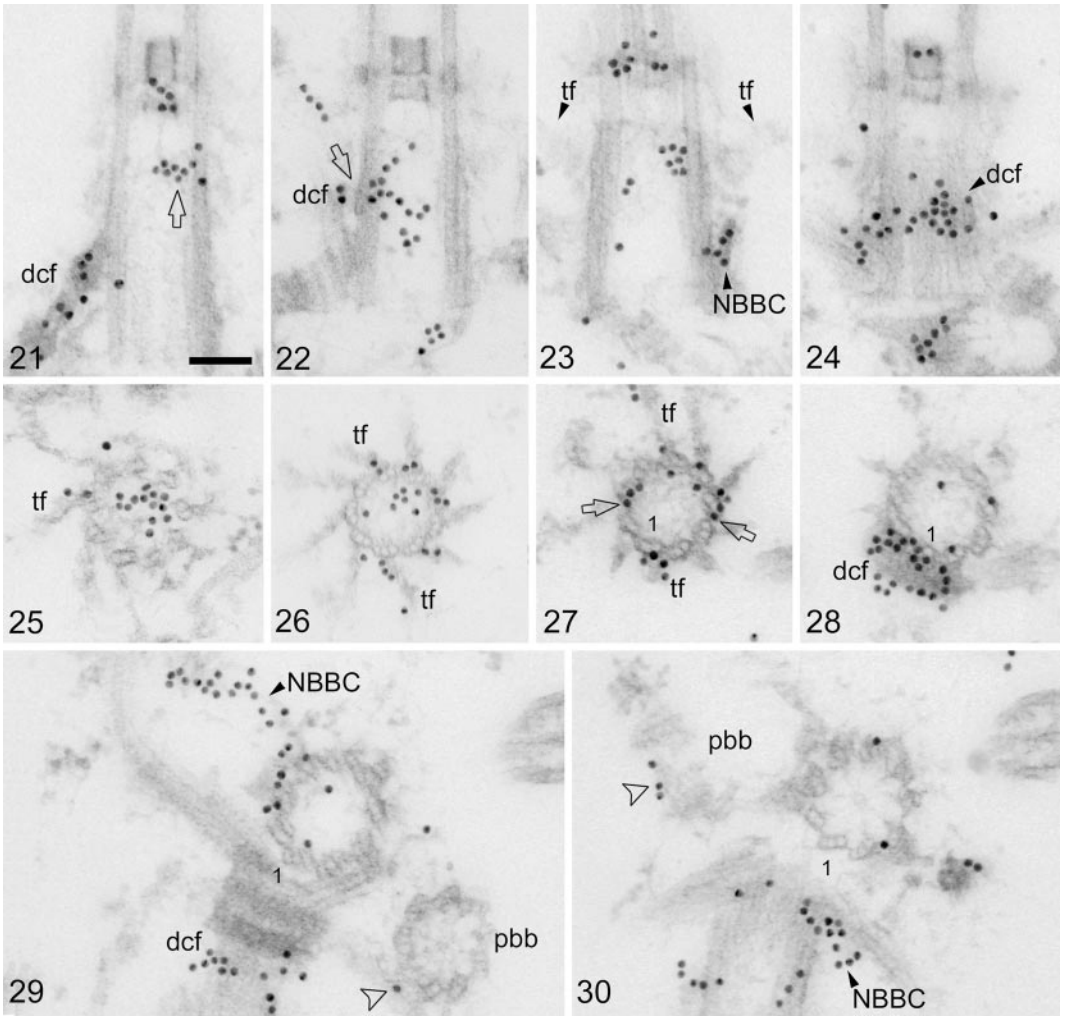

FIG. 2. Postembedding immunogold labeling of centrin (15-nm gold particles) in isolated cytoskeletons of *C. reinhardtii*. Scale bar: 0.1 μm. (21 and 22) Random longitudinal sections through basal bodies showing centrin labeling of the distal connecting fiber (dcf) and its interconnection with the V-shaped filament system (22; arrow). The upper (distal) part of the V-shaped filament system is also labeled with centrin (21; arrow). (23 and 24) Two consecutive longitudinal serial sections through a basal body depicting centrin labeling at the contact site of an NBBC with a basal body triplet (23; NBBC) and in the next section (a tangential section through the basal body) over the contact area of the distal connecting fiber with the basal body triplets (24; dcf). The contact areas of the NBBC and the distal connecting fiber are in close proximity as revealed by the centrin labeling (23 and 24). Two opposite transitional fibers (tf) in longitudinal section are visible in panel 23. The transitional fibers extend proximally towards the contact areas of the NBBC and the distal connecting fiber with the basal body triplets (23). (25 and 26) Random cross sections through the distal parts of basal bodies, revealing asymmetric centrin labeling in the basal body lumen presumably associated with the V-shaped filament system as well as centrin labeling in the transitional fibers (tf). (27 to 30) Serial cross sections through a basal body from its distal (27) to its proximal end (30) showing various centrin-labeled structures. Basal body triplet 1 is marked. Centrin labeling is depicted in the transitional fibers (27; tf), in the interlinkers between basal body triplets in the contact region of the transitional fibers with the basal body triplets (27; arrows), in the distal connecting fiber (28 and 29; dcf), in the basal body lumen (weak labeling in panels 28 to 30), in both NBBCs (29 and 30; NBBC), and at the distal end (surface) of a probasal body (in longitudinal section; 30; arrowhead; pbb). Centrin labeling (arrowhead in panel 29) also occurs at the junction of a probasal body (pbb) with the two-stranded microtubular flagellar root (the latter is more clearly seen in the following section [30]).

panel 37, and 5, panel 41). Additional thinner filaments connect the thick filaments also to triplets/doublets 3 and 6 (Fig. 4, panel 37, and 5, panel 41). In longitudinal sections through basal bodies the two V-shaped filaments are oriented almost perpendicular to the long axis of the basal body and in the center of the basal body lumen they are linked to the fine filament emanating from the flagellar transitional region (Fig. 1, panels 10, 11, and 20, and 5, panel 39). From the junction with the fine filament, the V-shaped filament system continues to extend further downwards (i.e., proximally), forming an angle of about 35° to the transverse basal body axis. The filament system traverses the lumen of the basal body, reaching the opposite surface almost 200 nm from its junction with the fine filament (Fig. 1, panels 10, 11, and 20, and 5, panel 39). At this basal body surface, the V-shaped filament system radiates into usually four separate fibers, which contact basal body triplets 8, 9, and 1 and the interlinkers to triplets 2 and 7 (Fig. 4, panel 38, and 5, panel 42). The V-shaped filament system contains centrin (Fig. 1, panels 7, 19, and 20, and 2, panels 21 to 23). Due to the oblique orientation of the V-shaped filament system (see above) centrin displays a rotationally asymmetric distribution in the distal part of the basal body. At the level of

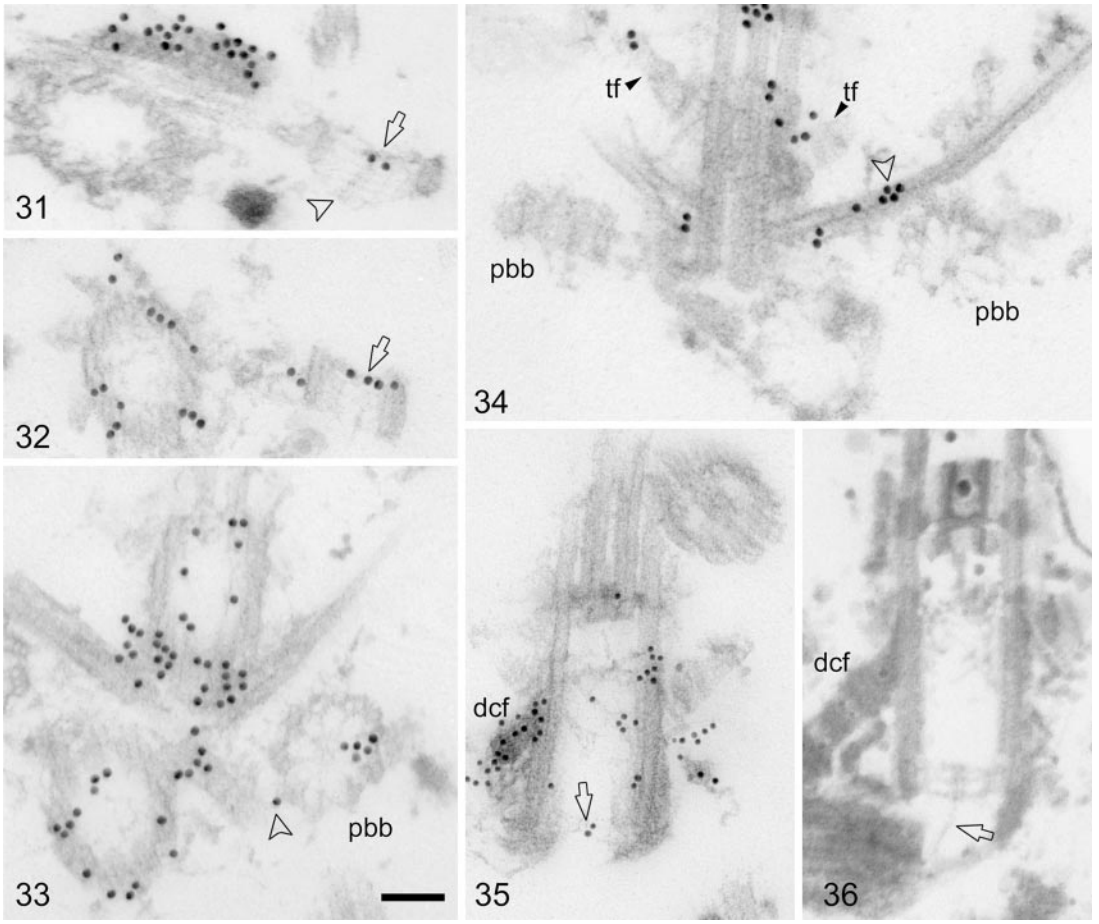

FIG. 3. Postembedding immunogold labeling of centrin in isolated cytoskeletons of *C. reinhardtii*. Shown are 15-nm gold particles (31 to 34), 10-nm gold particles (35), and cytoskeletons fixed and embedded for standard electron microscopy (36). Scale bar: 0.1 μm. (31 and 32) Two random longitudinal sections through probasal bodies revealing centrin labeling near the distal end (surface) of the probasal bodies (arrows). The arrowhead in panel 31 depicts a cartwheel extending from the proximal surface of the probasal body. (33) Cross section through flagellum-bearing basal bodies and a probasal body (pbb). Centrin labeling in the probasal body is asymmetric. Arrowhead, centrin labeling at the junction between the probasal body and the associated two-stranded microtubular root. (34) Section through both probasal bodies (pbb) of a basal apparatus. The left probasal body is longitudinally sectioned, and the right basal body is cross sectioned near its proximal end. A prominent "patch" of centrin labeling is seen at the junction between the cross-sectioned probasal body and the associated two-stranded microtubular flagellar root (arrowhead). Two opposite transitional fibers (tf), partly labeled, are visible. (35) Longitudinally sectioned basal body (the distal connecting fiber is labeled dcf) with a distinct but weak centrin labeling at the proximal end of the basal body near the central hub of the cartwheel (arrow). (36) Similar section to that depicted in panel 35 but from cytoskeletons fixed and embedded for standard electron microscopy body (the distal connecting fiber is labeled dcf). From the central hub of the the cartwheel in the longitudinally sectioned basal body extends a fine filament towards the proximal end of the opposite basal body (arrow).

the acorn, centrin is predominantly located in the part of the basal body lumen not containing the acorn (Fig. 2, panel 21, and 5, panel 41), whereas at a slightly lower (proximal) level, centrin is associated mostly with the opposite part of the basal body lumen underlying the acorn (Fig. 1, panel 20, 2, panel 22, and 5, panels 39 and 42). The asymmetric distribution of centrin is also evident in cross sections through the distal part of the basal body (Fig. 1, panel 13, and 2, panels 25 and 26).

Another novel localization of centrin in the basal apparatus is that of the transitional fibers (Fig. 1, panels 13, 14, and 17, 2, panels 25 to 27, and 5, panels 41 to 43). The nine fibers project radially and in counterclockwise orientation from each basal body triplet and in intact cells attach the basal bodies to the plasma membrane. They are associated with the triplets over a considerable length of the distal part of the basal bodies (Fig. 2, panel 23, and 5, panel 39). Since centrin labeling of the transitional fibers was not intensive, a statistical analysis of centrin distribution was performed (Table 1). In immune-labeled cross sections through basal bodies ($n = 54$) about 87% of the basal bodies revealed labeling of at least one transitional fiber (with an average labeling density of 1.8 gold particles/transitional fiber; on average 2.9 ± 1.3 [standard deviation] transitional fibers were labeled per basal body). In preimmune controls ($n = 34$) only 6% of the basal bodies displayed gold particles over transitional fibers (average labeling density: 1 gold particle/transitional fiber). Labeling was more prominent in the broader, proximal parts of the transitional fibers compared to the thinner distal parts (Fig. 1, panels 13, 14, and 17, and 2, panels 26 and 27) and also extended into the linkers interconnecting basal body triplets (Fig. 1, panels 14 and 17, and 2, panel 27).

Of the remaining centrin localizations in the basal appara-

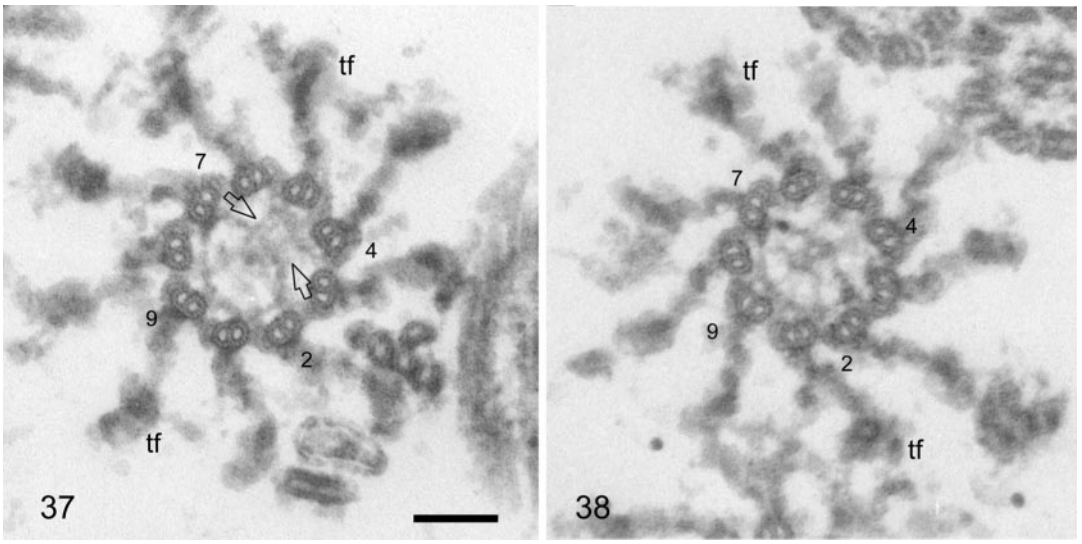

FIG. 4. Random cross sections through the distal parts of basal bodies from cytoskeletons fixed and embedded for standard electron microscopy. Scale bar: 0.1 μm. Basal body doublets/triplets 2, 4, 7, and 9 are numbered, and some transitional fibers (tf) are marked. The left section is slightly more distal than the right, but both show the "acorn" in the lower left part of the basal body lumen attached to doublets/triplets 7, 8, 9, 1, and 2. The V-shaped filament system occupies the area opposite the acorn in the more distal section (arrows in panel 37), whereas, in the more proximal section (38), it extends into the area of the acorn (actually slightly proximal to the acorn; see also Fig. 5, panels 39 to 44), radiating into several thin filaments which link to doublets/triplets 8, 9, and 1. For a schematic representation of the acorn and V-shaped filament system seen in panels 37 and 38, see Fig. 5, panels 41 and 42, respectively. To be consistent with the other schematic drawings, the basal bodies have been rotated counterclockwise by 90° compared to the basal bodies shown in panels 37 and 38.

tus, the two most prominent were the distal connecting fiber and the nucleus-basal body connectors, two well-known centrin-containing structures. In our preparations, the most heavily labeled basal apparatus component was the distal connecting fiber (Fig. 1, panels 10, 15, 16, 19, and 20, 2, panel 21, and 3, panels 31, 33, and 35). The distal connecting fiber is cross-striated and interconnects the two flagellum-bearing basal bodies (Fig. 1, panel 11, 2, panel 29, and 5, panel 39). Although there was some indication that centrin labeling was more prominent over the electron-dense striations compared to the more lightly staining regions of the fiber (Fig. 1, panels 10 and 20, and 2, panel 21), we did not investigate this in a quantitative manner. Of greater interest in the present context was the observation that centrin labeling in the distal connecting fiber apparently extends into the basal body lumen and is continuous with the downward-bending part of the V-shaped filament system. This is most clearly documented in longitudinal sections through basal bodies (Fig. 1, panels 19 and 20, and 2, panel 22); but that centrin labeling from the distal connecting fiber extends at least into the linkers between basal body triplets 9, 1, and 2 was also observed in cross sections through basal bodies (Fig. 2, panel 28). Serial cross sections, however, due to the oblique orientation of the V-shaped filament system in the basal body lumen (see above), cannot reveal the continuity between the distal connecting fiber and the V-shaped filament system (Fig. 1, panels 13 to 15).

The two NBBCs extend from the flagellum-bearing basal bodies and connect the basal apparatus with the nucleus. In

TABLE 1. Postembedding immunogold labeling of centrin in isolated cytoskeletons of *Chlamydomonas reinhardtii*

Parameter	Value for:			
	Axoneme	Transitional region	Transitional fibers[b]	Probasal body
Immune labeling				
n[a]	536	39	54	93
% Labeled (*n*)	41.6 (223)	84.6 (33)	87.0 (47)	61.3 (57)
% Unlabeled (*n*)	58.4 (313)	15.4 (6)	13.0 (7)	38.7 (36)
Avg labeling density (SD)	1.8 (0.9)	9.9 (4.2)	1.8 (1.4)	3.5 (2.0)
Preimmune labeling				
n	334	35	34	115
Labeled	5.7 (19)	2.9 (1)	5.9 (2)	6.9 (8)
Unlabeled	94.3 (315)	97.1 (34)	94.1 (32)	93.1 (107)
Avg labeling density (SD)	1.4 (0.6)	1 (0)	1 (0)	1.2 (0.4)

[a] *n*, total number of randomly chosen cross sections through axonemes, basal bodies, and probasal bodies which were used to determine centrin labeling over four cytoskeletal structures.

[b] For transitional fibers centrin labeling was counted positive if at least one of the nine transitional fibers were labeled in a basal body cross section. The average labeling density of the transitional fibers refers to the number of gold particles/individual transitional fiber.

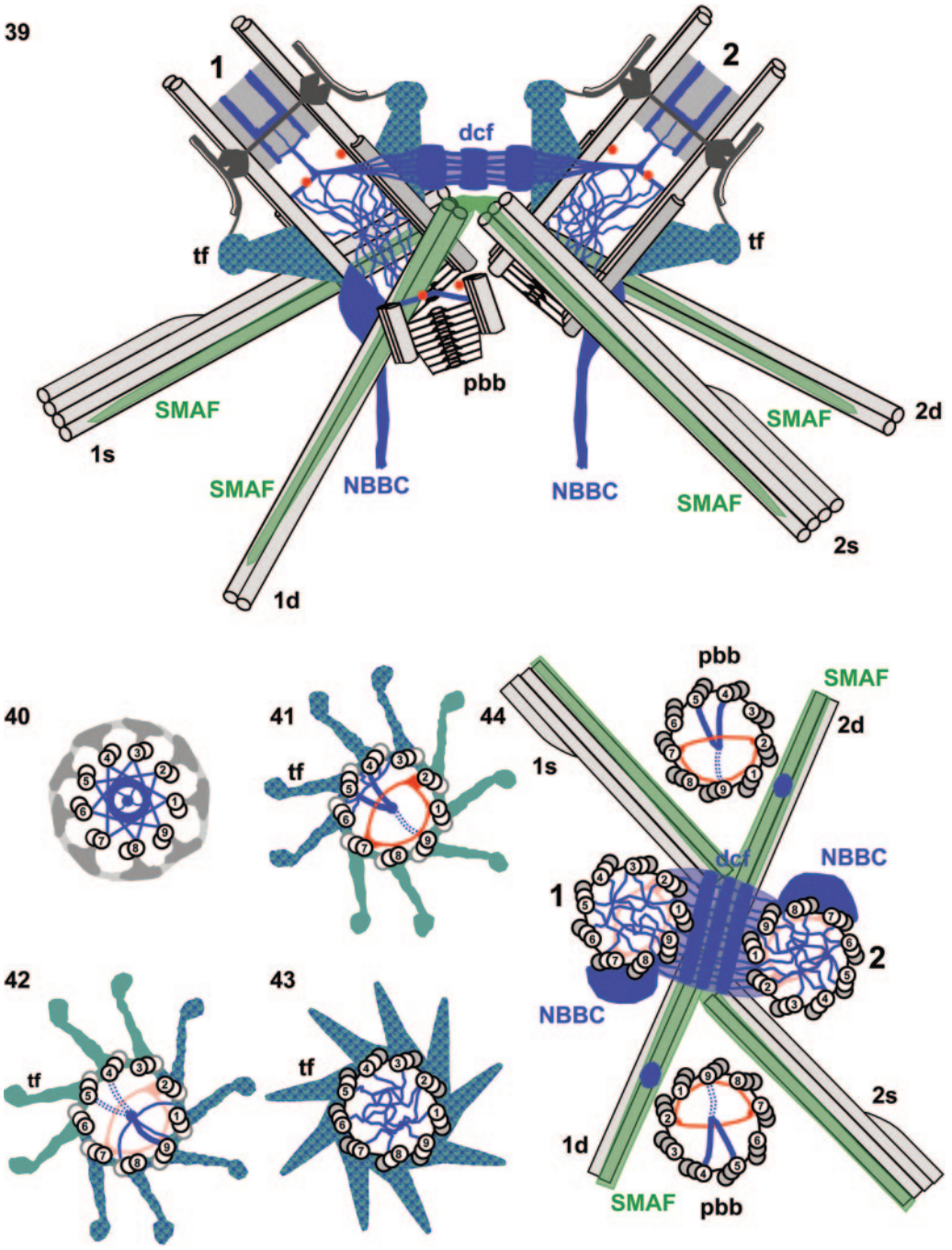

FIG. 5. Schematic presentation of centrin distribution (blue) in the basal apparatus of *Chlamydomonas reinhardtii* based on preembedding serial section immunogold localization of centrin in isolated cytoskeletons. (39) Basal apparatus with the two flagellum-bearing basal bodies in longitudinal sections (no. 1 for the older basal body and no. 2 for the younger basal body), including the transitional regions of the axonemes, one of the two probasal bodies (pbb), the distal connecting fiber (dcf) linking the two basal bodies, and the four flagellar roots with their microtubular (1s, 1d, 2s, and 2d; light gray) and fibrous (SMAF [striated microtubule-associated fibers]; green) components. The centrin-containing structures form a continuous filamentous scaffold that extends from the two NBBCs through the basal bodies to the transitional region of the axonemes and includes the transitional fibers (tf). In the distal part of the basal bodies and the probasal body, "acorns" (13) are depicted in cross sections (two red dots). In the same area of each basal body, the centrin-containing V-shaped filament systems (blue lines that intersect the central red dot) and their continuity with the dcf as well as their connection with the transitional regions and the centrin-containing filaments in the basal body lumen are shown. (40 to 43) Serial cross sections through axonemes/basal bodies from the flagellar transitional region (40) to the distal part of the basal bodies (43). The axonemal/basal body doublets/triplets are numbered. Centrin is shown in blue and the acorn in red. Note the asymmetric distribution of centrin in the basal body lumen in the region of the acorn (41 and 42). A continuity of centrin-containing filaments between the V-shaped filament system (41 and 42) and the transitional fibers (tf) is assumed to occur through the interdoublet/triplet linkers. (44) Cross section through a basal apparatus depicting all four basal bodies (the two flagellum-bearing basal bodies [no. 1 and 2] and two probasal bodies [pbb]; the triplets are numbered) and the four flagellar roots (for abbreviations and color coding, see legend to panel 39). Centrin localization (blue) is shown in the distal connecting fiber (dcf), the NBBC, and the basal body lumen, and acorns are depicted in red. The asymmetric distribution of the V-shaped filament system in the probasal bodies is indicated, as well as a prominent "patch" of centrin on the surface of the two-stranded microtubular roots near their junction with the probasal bodies.

our preparations nuclei were often detached from the basal apparatuses and thus NBBCs were sometimes inconspicuous. We verified that the proximal end of the NBBC is associated with basal body triplets 7 and 8 (Fig. 1, panel 16, 2, panel 29, and 5, panel 44). Serial sections through basal bodies (both longitudinal and cross sections) in the area of association of the NBBC with the basal body indicated that the NBBC comes into very close (<50 nm) contact with two other centrin-containing structures, namely, the distal connecting fiber (Fig. 2, panels 23, 24, 28, and 29) and the transitional fibers (Fig. 1, panels 15 and 16). Because the distal connecting fiber inserts at basal body triplet 9 slightly (30 to 40 nm) above (i.e., distal to) the NBBC (Fig. 2, panels 23 and 24), a direct continuity of these two centrin-containing structures was difficult to prove in serial cross sections through basal bodies (Fig. 1, panels 15 and 16, and 2, panels 28 to 30). The same holds true for the association of the proximal base of two transitional fibers (those linked to triplets 7 and 8) and the NBBC (Fig. 1, panels 15 and 16, and 2, panel 23 [longitudinal section]). These centrin-containing structures touch each other at the basal body surface (Fig. 2, panel 23); however, because of the weak centrin labeling of the transitional fibers (see above), no continuity in the distribution of gold particles between the two structures could be shown.

Finally, centrin labeling was also found in the central and proximal parts of the basal body lumen (Fig. 1, panels 7 to 10, 2, panels 22, 23, and 28 to 30, and 3, panel 35). We have previously shown that the basal body lumen of isolated *Chlamydomonas reinhardtii* cytoskeletons contains filaments, some of which are attached to the A-tubule feet at the inner surface of the triplets (13). The quantity of these filaments varied among basal bodies, suggesting differential extraction of filaments during isolation or preparation of cytoskeletons for electron microscopy. Thus, no attempt was made to quantify the labeling or analyze its distribution. We note, however, that the basal body lumen reveals centrin labeling in the area where the NBBC is linked to triplets 7 and 8 (Fig. 1, panel 16, and 2, panel 29) and that a peculiar centrin localization was observed on several occasions at the proximal end of a basal body near the central hub of the cartwheel from which a fine filament extends towards the proximal end of the opposite basal body (Fig. 3, panels 35 and 36).

In addition to the flagellum-bearing basal bodies, most basal apparatuses of isolated cytoskeletons also contained two probasal bodies (Fig. 2, panels 29 and 30, 3, panel 34, and 5, panels 39 and 44 [schematic presentation]). Probasal bodies are very short (about 100 nm in length) (13) and consist of a microtubular cylinder of nine triplets and an elaborate cartwheel which fills the lumen of the probasal body almost completely and protrudes proximally from the microtubular triplets in a conical shape (Fig. 3, panel 31). The distal end of a probasal body contains an acorn (13) (Fig. 5, panels 39 and 44). Here we show that centrin is present in the probasal bodies (Fig. 2, panel 30, and 3, panels 31 to 33). In immune-labeled cross sections through probasal bodies ($n = 93$) 61% of the probasal bodies displayed gold particles (with an average labeling density of 3.5 gold particles/probasal body; Table 1). In preimmune controls only 7% of the probasal bodies ($n = 115$) were labeled with gold particles (average labeling density: 1.2 gold particles/probasal body). Centrin labeling was exclusively confined to the distal end of the probasal bodies, as shown in longitudinal sections through probasal bodies (Fig. 2, panel 30, and 3, panels 31 and 32). In cross sections through probasal bodies ($n = 59$) centrin labeling was rotationally asymmetric, with twice as many probasal bodies (54%) labeled in the luminal part opposite the acorn compared to the luminal part containing the acorn (24%; label in the remaining probasal bodies was distributed equally over both luminal parts). We have previously shown that probasal bodies contain the typical V-shaped filament system near their distal end (13) (see also schematic presentations in Fig. 5, panels 39 and 44). We also searched for a centrin connective between probasal bodies and the flagellum-bearing basal bodies, but without success. However, we consistently observed a centrin "patch" on the two-stranded microtubular flagellar root near the site where the probasal body is attached to the two-stranded root (Fig. 2, panel 29, 3, panels 33 and 34, and 5, panel 44 [schematic presentation]).

The various centrin localizations in the basal apparatus of isolated cytoskeletons of *Chlamydomonas reinhardtii* documented in this study by postembedding serial section immunoelectron microscopy are summarized in the schematic presentations of Fig. 5, panels 39 to 44. Our interpretation of the distribution of centrin in the basal apparatus of *Chlamydomonas reinhardtii* is that centrin is intimately associated with a complex filamentous network which pervades the basal apparatus and extends from the nuclear surface to the proximal end of the flagella and is here termed the centrin scaffold.

DISCUSSION

The distribution of centrin in the basal apparatus of the flagellate green alga *Chlamydomonas reinhardtii* has been studied in detail by serial section postembedding immunoelectron microscopy of cytoskeletons isolated from interphase cells. Although centrin was first discovered in a flagellate green alga (60) and its localization in the basal apparatus of algae has been well investigated at both the light microscopy and electron microscopy levels (reviewed in reference 44), several novel centrin localizations were discovered during the course of this study. Since centrin was localized in isolated cytoskeletons, the likelihood of an artificial association of centrin with basal apparatus components during cell disruption should be considered. We have previously shown that the basal apparatus of isolated cytoskeletons of *C. reinhardtii* remains structurally intact and that its detailed ultrastructure corresponds to that of the in situ basal apparatus (13). Several functions of the basal apparatus have been reconstituted in isolated cytoskeletons such as the contraction of the centrin-containing NBBCs (77), and we have confirmed all previously known in situ localizations of centrin in *C. reinhardtii* (61) also in the isolated cytoskeletons. Searching published micrographs for the novel centrin localizations in *C. reinhardtii* yielded a positive hit for the distal part of the basal body lumen (Fig. 4 in reference 61 and 6A in reference 63 [both in situ localizations]). That the distal parts of basal bodies/centrioles contain centrin was first described in brown algal gametes (24), but later also documented from amoeboflagellates to humans (37, 49). It is likely that centrin is located in the distal lumen of the basal body/centriole in most if not all eukaryotes. The presence of centrin in novel localizations in the *Chlamydomonas* basal apparatus is

thus most likely not caused by the attraction of soluble centrin to basal apparatus components during cell disruption, but is genuine. However, the possibility of an artificial redistribution of centrin during cell disruption could be excluded by an investigation of cryofixed whole cells, which would also allow the localization of possible pools of soluble centrin within the cell/in the vicinity of the basal apparatus.

The failure to recognize centrin as a component of the basal body proper in *Chlamydomonas* (see, e.g., reference 28) is likely related to the preponderance of the preembedding technique (which precludes access of gold particles to the basal body lumen) and the difficulty to distinguish false positives from true centrin labeling when labeling is weak and fixation/contrast suboptimal as in many previous postembedding studies. An additional advantage of using isolated cytoskeletons is that the high density of basal apparatuses supports a statistical approach which significantly increases the confidence level of even weak labeling densities. When isolated cytoskeletons of *C. reinhardtii* were recently used to establish a high-resolution structural map of the interphase basal apparatus, it was anticipated that the data would "facilitate the precise mapping of previously identified basal apparatus proteins" (13). This expectation was confirmed upon probing centrin localization in isolated cytoskeletons: in the distal part of the basal body, centrin was found to be associated with a specific rotationally asymmetric structure, the V-shaped filament system, which had been discovered during the previous study. Interestingly, both the V-shaped filament system and centrin are already present in the "dormant" probasal bodies of *C. reinhardtii* (reference 13 and this study), suggesting that the V-shaped filament system is the essential centrin-containing structure of a developing basal body. In various other systems, centrin has been found to be associated with developing (nascent) basal bodies/centrioles (reviewed in reference 5), e.g., in the blepharoplast of *Marsilea* (26), in fibrogranular precursors of centrioles of human epithelial cells (29, 30), and at the surface of fibrous probasal body precursors in flagellate green algae (31). In addition, functional/genetic evidence has been accumulating that centrin is involved in basal body assembly/duplication (28, 46, 49, 62). It is thus possible that the V-shaped filament system or its precursor in conjunction with other proteins is involved in probasal body formation/assembly.

Centrin has also been discovered in the transitional fibers. The transitional fibers have been inferred to function as docking sites for intraflagellar transport particles and their motors destined for the flagella (9). Intraflagellar transport (IFT) is required for the assembly and maintenance of flagella and involves the transport of non-membrane-bound macromolecular protein complexes (IFT particles) from the cell body to the tip of the flagellum and back (reviewed in references 56 and 66). Interestingly, centrin is known as a light chain associated with one type of inner dynein arm in axonemes of *C. reinhardtii* (33, 52) and has been implicated in different ciliary functions (14, 15). Here, we have shown specific centrin labeling of outer axonemal doublets consistent with the biochemical evidence. However, the centrin labeling density of both the axonemes and the transitional fibers was relatively low (see Results). Loss of centrin during isolation of the cytoskeletons and/or preparatory steps for electron microscopy may be one explanation for the observed weak labeling. In isolated mammalian centrosomes, centrin is only extracted when drastic conditions such as 8 M urea or high temperatures (45°C) are applied (49). One of the inner dynein arm complexes (2B) containing centrin, however, was shown to be extracted by low concentrations of the detergent Nonidet P-40 (33). It is thus conceivable that, depending on whether centrin is associated with (contractile) filaments or is part of a heavy-chain dynein complex, it may be differentially stable to extraction. The weak centrin labeling of the transitional fibers may be related to extraction of cargo centrin in transit to the IFT machinery (the latter appears to be concentrated at the distal ends of the transitional fibers [9]). There is strong evidence that inner dynein arm subunits are transported in and out of the flagellum by IFT. Inactivation of the anterograde IFT motor kinesin II blocks the normal addition of inner dynein arms onto existing outer doublet microtubules, presumably because, in the absence of IFT, these components are not transported to the tip where flagellar assembly occurs (51). More direct evidence comes from coimmunoprecipitation experiments showing that several subunits of inner dynein arms interact with IFT particles (54). Centrin, in its function as light chain of one type of inner dynein arm as well might bind to and be transported by IFT particles.

Alternatively, the weak centrin labeling of the transitional fibers may represent the distal ramifications of the centrin scaffold (see below).

The most significant single observation made during this study is that the previously distinct centrin localizations in the *Chlamydomonas* basal apparatus are part of a continuous centrin scaffold (see Results and Fig. 5, panels 39 to 44). It is well known that in many protists centrin is part of a contractile filament system which can be as elaborate as the striated flagellar roots (rhizoplasts) of *Tetraselmis* (from which centrin was originally isolated [60]), the paraxonemal rod of the dinoflagellate transverse flagellum (16), or the spasmoneme of vorticellid ciliates (1). The unique contraction cycle of this filament system, consisting of rapid contractions and slow extensions, has been regarded as representing a novel cell motility mechanism in eukaryotes distinct from the sliding-filament mechanisms of actomyosin or microtubule/dynein (43, 57). The main centrin localizations in the *Chlamydomonas* basal apparatus have also been shown to be filamentous and contractile (reviewed in reference 44). The algal centrin molecule, when expressed heterologously in *Escherichia coli*, forms Ca^{2+}-dependent multimers in vitro which display a network of filaments with a diameter of ~30 nm (76). In vitro studies of human centrin 2 (HsCen2) corroborated these results and revealed reversible self-assembly resembling nucleation-controlled polymerization (74). A truncated form of HsCen2 lacking the N-terminal 25 amino acids showed no detectable self-assembly, suggesting that the N terminus of centrin is necessary for centrin-centrin interactions. While it was often discussed whether centrin alone might form the 3- to 7-nm contractile filaments in vivo, this appears now unlikely with the recent discovery in yeasts and humans of Sfi1p, a protein containing 17 to 23 internal novel repeats (termed Sfi1 repeats [25]), each of which apparently binds one centrin molecule. Since the Sfi1 repeats generally lack prolines, they might adopt a helical confirmation and Sfi1p may be a filamentous monomer forming a template on which centrin molecules can polymerize (25). According to

one model, the Sfi1p-centrin complex is a two-component molecular thread with Sfi1p serving as a flexible elastic backbone. Upon binding of Ca^{2+}, conformational changes in centrin molecules, which remain bound to Sfi1p, may lead to torsion forces causing the Sfi1p-centrin complex to bend, twist, or supercoil (25, 59). The polymerization of Sfi1p into larger filaments, however, remains to be demonstrated. In the flagellate green alga *Spermatozopsis similis*, a protein of 92.4 kDa (CBP1.1) containing 18 Sfi1 repeats of 33 amino acids each was discovered in a cDNA expression library probed with a centrin overlay (71; J. Steinkötter, unpublished observations). It is therefore likely that the centrin scaffold of *C. reinhardtii* contains Sfi1p/CBP1.1 in addition to centrin and thus represents the Ca^{2+}-sensitive contractile protein machinery of the basal apparatus.

The presence of a centrin scaffold readily explains the various centrin localizations found previously in the basal apparatus without the need to postulate that the specificity of centrin localization is determined by specific centrin-binding proteins. The occurrence of a filamentous centrin "seed" in probasal bodies (i.e., the V-shaped filament system) provides an elegant mechanism by which the centrin scaffold may grow with the developing basal body by addition of monomers. Basal bodies and centrioles display longitudinal and circumferential polarities, and a variety of proteins have been shown to be localized in an asymmetric manner to the outside of the microtubular cylinder (4). The only other protein besides centrin (this study) shown to be localized in a rotational asymmetric manner within the microtubular cylinder of the basal body in *Chlamydomonas* is VFL1p. VFL1p has been shown to be localized at the most distal end of the basal body within the half that faces the distal connecting fiber and contains triplets 9, 1, and 2 (68). This localization corresponds well with the position of the acorn and suggests that VFL1p might be a component of this structure. Like centrin, Vlf1p is already present at the probasal body. The centrin seed (together with the acorn [13]) provides rotational asymmetry to the developing basal body (see Results), and the interplay between the acorn and the centrin "seed" may determine which microtubular triplets become associated with the centrin-containing filaments during maturation of the probasal body and at which level this occurs in the basal body lumen.

We have been unable to detect a centrin-containing filamentous linkage between the parental basal bodies and the probasal bodies in the isolated cytoskeletons. A delicate linkage may have been severed during isolation of cytoskeletons and/or additional preparatory steps for electron microscopy. Alternatively, such a centrin linker may not exist during interphase, when probasal bodies are in a "dormant" status. In *Spermatozopsis similis*, a transient centrin linker was reported to be present only during the first stages of probasal development (31). How probasal bodies in *C. reinhardtii* recruit their centrin "seeds" is thus currently unknown and must await an analysis of centrin localization during mitosis, when new probasal bodies are formed. We note, however, that a "patch" of centrin was consistently observed on the two-stranded microtubular flagellar roots (d roots) near the docking site of the probasal bodies (see Results) and may relate to a "store of centrin," perhaps to be used on a later occasion. During mitosis the parental distal connecting fiber is disassembled (it is a bipolar structure that presumably dissociates in the center). During interphase, probasal bodies are oriented in such a way that their triplets 9, 1, and 2 are adjacent to the parental distal connecting fiber (13) (Fig. 5, panel 44). Growth of the two centrin scaffolds (from the parental and the probasal body) towards each other could thus reestablish the bipolar nature of the distal connecting fiber in the progeny basal apparatus (for an alternative view about the formation of the distal connecting fiber, see reference 32).

ACKNOWLEDGMENTS

This work was supported by the Deutsche Forschungsgemeinschaft (Me 658/22-2) and the University of Cologne.

We thank Siegfried Werth for help in the preparation of the plates and Dennis Diener for critical reading of the manuscript.

REFERENCES

1. **Amos, W. B., L. M. Routledge, and F. F. Yew.** 1975. Calcium-binding proteins in a vorticellid contractile organelle. J. Cell Sci. **19:**203–213.
2. **Araki, M., C. Masutani, M. Takemura, A. Uchida, K. Sugasawa, J. Kondoh, Y. Ohkuma, and F. Hanaoka.** 2001. Centrosome protein centrin 2/caltractin 1 is part of the xeroderma pigmentosum group C complex that initiates global genome nucleotide excision repair. J. Biol. Chem. **276:**18665–18672.
3. **Baum, P., C. Furlong, and B. Byers.** 1986. Yeast gene required for spindle pole body duplication: homology of its product with $Ca2^{+}$-binding proteins. Proc. Natl. Acad. Sci. USA **83:**5512–5516.
4. **Beisson, J., and M. Jerka-Dziadosz.** 1999. Polarities of the centriolar structure: morphogenetic consequences. Biol. Cell **91:**367–378.
5. **Beisson, J., and M. Wright.** 2003. Basal body/centriole assembly and continuity. Curr. Opin. Cell Biol. **15:**96–104.
6. **Bhattacharya, D., J. Steinkötter, and M. Melkonian.** 1993. Molecular cloning and evolutionary analysis of the calcium-modulated contractile protein, centrin, in green algae and land plants. Plant Mol. Biol. **23:**1243–1254.
7. **Biggins, S., and M. D. Rose.** 1994. Direct interaction between yeast spindle pole body components: Kar1p is required for Cds31p localization to the spindle pole body. J. Cell Biol. **125:**843–852.
8. **Cox, J. A., F. Tirone, I. Durussel, C. Firanescu, Y. Blouquit, P. Duchambon, and C. T. Craescu.** 2005. Calcium and magnesium binding to human centrin 3 and interaction with target peptides. Biochemistry **44:**840–850.
9. **Deane, J. A., D. G. Cole, E. S. Seeley, D. R. Diener, and J. L. Rosenbaum.** 2001. Localization of intraflagellar transport protein IFT52 identifies basal body transitional fibers as the docking site for IFT particles. Curr. Biol. **11:**1586–1590.
10. **Errabolu, R., M. A. Sanders, and J. L. Salisbury.** 1994. Cloning of a cDNA encoding human centrin, an EF-hand protein of centrosomes and mitotic spindle poles. J. Cell Sci. **107:**9–16.
11. **Fischer, T., S. Rodríguez-Navarro, G. Pereira, A. Rácz, E. Schiebel, and E. Hurt.** 2004. Yeast centrin Cdc31 is linked to the nuclear mRNA export machinery. Nat. Cell Biol. **6:**840–848.
12. **Gavet, O., C. Alvarez, P. Gaspar, and M. Bornens.** 2003. Centrin4p, a novel mammalian centrin specifically expressed in ciliated cells. Mol. Biol. Cell **14:**1818–1834.
13. **Geimer, S., and M. Melkonian.** 2004. The ultrastructure of the *Chlamydomonas reinhardtii* basal apparatus: identification of an early marker of radial asymmetry inherent in the basal body. J. Cell Sci. **117:**2663–2674.
14. **Gonda, K., A. Yoshida, K. Oami, and M. Takahashi.** 2004. Centrin is essential for the activity of the ciliary reversal-coupled voltage-gated Ca^{2+} channels. Biochem. Biophys. Res. Commun. **323:**891–897.
15. **Guerra, C., Y. Wada, V. Leick, A. Bell, and P. Satir.** 2003. Cloning, localization, and axonemal function of *Tetrahymena* centrin. Mol. Biol. Cell **14:**251–261.
16. **Höhfeld, I., J. Otten, and M. Melkonian.** 1988. Contractile eukaryotic flagella: centrin is involved. Protoplasma **147:**16–24.
17. **Höhfeld, I., P. L. Beech, and M. Melkonian.** 1994. Immunolocalization of centrin in *Oxyrrhis marina*. J. Phycol. **30:**474–489.
18. **Hoops, H. J., and G. B. Witman.** 1983. Outer doublet heterogeneity reveals structural polarity related to beat direction in *Chlamydomonas* flagella. J. Cell Biol. **97:**902–908.
19. **Hu, H., and W. J. Chazin.** 2003. Unique features in the C-terminal domain provide caltractin with target specificity. J. Mol. Biol. **330:**473–484.
20. **Hu, H., J. H. Sheehan, and W. J. Chazin.** 2004. The mode of action of centrin. Binding of Ca^{2+} and a peptide fragment of Kar1p to the C-terminal domain. J. Biol. Chem. **279:**50895–50903.
21. **Huang, B., A. Mengersen, and V. D. Lee.** 1988. Molecular cloning of cDNA for caltractin, a basal body-associated Ca^{2+}-binding protein: homology in its protein sequence with calmodulin and the yeast CDC31 gene product. J. Cell Biol. **107:**133–140.
22. **Huang, B., D. M. Watterson, V. D. Lee, and M. J. Schibler.** 1988b. Purifi-

cation and characterization of a basal body-associated Ca^{2+}-binding protein. J. Cell Biol. **107:**121–131.
23. **Jaspersen, S. L., T. H. Giddings, Jr., and M. Winey.** 2002. Mps3p is a novel component of the yeast spindle pole body that interacts with the yeast centrin homologue Cdc31p. J. Cell Biol. **159:**945–956.
24. **Katsaros, C. I., I. Maier, and M. Melkonian.** 1993. Immunolocalization of centrin in the flagellar apparatus of male gametes of *Ectocarpus siliculosus* (*Phaeophyceae*) and other brown algal motile cells. J. Phycol. **29:**787–797.
25. **Kilmartin, J. V.** 2003. Sfi1p has conserved centrin-binding sites and an essential function in budding yeast spindle poly body duplication. J. Cell Biol. **162:**1211–1221.
26. **Klink, V., and S. Wolniak.** 2001. Centrin is necessary for the formation of the motile apparatus in spermatids of *Marsilea*. Mol. Biol. Cell **12:**761–776.
27. **Klotz, C., N. Garreau de Loubresse, F. Ruiz, and J. Beisson.** 1997. Genetic evidence for a role of centrin-associated proteins in the organization and dynamics of the infraciliary lattice in *Paramecium*. Cell Motil. Cytoskelet. **38:**172–186.
28. **Koblenz, B., J. Schoppmeier, A. Grunow, and K.-F. Lechtreck.** 2003. Centrin deficiency in *Chlamydomonas* causes defects in basal body replication, segregation and maturation. J. Cell Sci. **116:**2635–2646.
29. **Laoukili, J., E. Perret, S. Middendorp, O. Houcine, C. Guennou, F. Marano, M. Bornens, and F. Tournier.** 2000. Differential expression and cellular distribution of centrin isoforms during human ciliated cell differentiation in vitro. J. Cell Sci. **113:**1355–1364.
30. **La Terra, S., C. N. English, P. Hergert, B. F. McEwen, G. Sluder, and A. Khodjakow.** 2005. The de novo centriole assembly pathway in HeLa cells: cell cycle progression and centriole assembly/maturation. J. Cell Biol. **168:** 713–722.
31. **Lechtreck, K.-F., and A. Grunow.** 1999. Evidence for a direct role of nascent basal bodies during spindle pole initiation in the green alga *Spermatozopsis similis*. Protist **150:**163–181.
32. **Lechtreck, K.-F., and M. Bornens.** 2001. Basal body replication in green algae—when and where does it start? Eur. J. Cell Biol. **80:**631–641.
33. **LeDizet, M., and G. Piperno.** 1995. The light chain p28 associates with a subset of inner dynein arm heavy chains in *Chlamydomonas* axonemes. Mol. Biol. Cell **6:**697–711.
34. **LeDizet, M., J. C. Beck, and W. E. Finkbeiner.** 1998. Differential regulation of centrin genes during ciliogenesis in human tracheal epithelial cells. Am. J. Physiol. **275:**L1145–L1156.
35. **Lee, V. D., and B. Huang.** 1993. Molecular cloning and centrosomal localization of human caltractin. Proc. Natl. Acad. Sci. USA **90:**11039–11043.
36. **Lemullois, M., G. Fryd-Versavel, and A. Fleury-Aubusson.** 2004. Localization of centrins in the hypotrich ciliate *Paraurostyla weissei*. Protist **155:**331–346.
37. **Levy, Y. Y., E. Y. Lai, S. P. Remillard, M. B. Heintzelman, and C. Fulton.** 1996. Centrin is a conserved protein that forms diverse associations with centrioles and MTOCs in *Naegleria* and other organisms. Cell Motil. Cytoskelet. **33:**298–323.
38. **Madeddu, L., C. Klotz, J.-P. Le Caer, and J. Beisson.** 1996. Characterization of centrin genes in *Paramecium*. Eur. J. Biochem. **238:**121–128.
39. **Marshall, W. F., Y. Vucica, and J. L. Rosenbaum.** 2001. Kinetics and regulation of de novo centriole assembly. Implications for the mechanism of centriole duplication. Curr. Biol. **11:**308–317.
40. **Matei, E., S. Miron, Y. Blouquit, P. Duchambon, I. Durussel., J. A. Cox, and C. T. Craescu.** C-terminal half of human centrin 2 behaves like a regulatory EF-hand domain. Biochemistry **42:**1439–1450.
41. **McFadden, G. I., and M. Melkonian.** 1986. Use of HEPES buffer for microalgal culture media and fixation for electron microscopy. Phycologia **25:** 551–557.
42. **McFadden, G. I., D. Schulze, B. Surek, J. L. Salisbury, and M. Melkonian.** 1987. Basal body reorientation mediated by a Ca^{2+}-modulated contractile protein. J. Cell Biol. **105:**903–912.
43. **Melkonian, M.** 1989. Centrin-mediated motility: a novel cell motility mechanism in eukaryotic cells. Bot. Acta **102:**3–4.
44. **Melkonian, M., P. L. Beech, C. Katsaros, and D. Schulze.** 1992. Centrin-mediated cell motility in algae, p. 179–221. *In* M. Melkonian (ed.), Algal cell motility. Chapman & Hall, New York, N.Y.
45. **Middendorp, S., A. Paoletti, E. Schiebel, and M. Bornens.** 1997. Identification of a new mammalian centrin gene, more closely related to *Saccharomyces cerevisiae* CDC31 gene. Proc. Natl. Acad. Sci. USA **94:**9141–9146.
46. **Middendorp, S., T. Küntziger, Y. Abraham, S. Holmes, N. Bordes, M. Paintrand, A. Paoletti, and M. Bornens.** 2000. A role for centrin 3 in centrosome reproduction. J. Cell Biol. **148:**405–415.
47. **Molinier, J., C. Ramos, O. Fritsch, and B. Hohn.** 2004. Centrin2 modulates homologous recombination and nucleotide excision repair in *Arabidopsis*. Plant Cell **16:**1633–1643.
48. **O'Toole, E. T., T. H. Giddings, J. R. McIntosh, and S. K. Dutcher.** 2003. Three-dimensional organization of basal bodies from wild-type and δ-tubulin deletion strains of *Chlamydomonas reinhardtii*. Mol. Biol. Cell **14:**2999–3012.
49. **Paoletti, A., M. Moudjou, M. Paintrand, J. L. Salisbury, and M. Bornens.** 1996. Most of centrin in animal cells is not centrosome-associated and centrosomal centrin is confined to the distal lumen of centrioles. J. Cell Sci. **109:**3089–3102.
50. **Paoletti, A., N. Bordes, R. Haddad, C. L. Schwartz, F. Chang, and M. Bornens.** 2003. Fission yeast cdc31p is a component of the half-bridge and controls SPB duplication. Mol. Biol. Cell **14:**2793–2808.
51. **Piperno, G., K. Mead, and S. Henderson.** 1996. Inner dynein arms but not outer dynein arms require the activity of kinesin homologue protein $KHP1^{FLA10}$ to reach the distal part of flagella in *Chlamydomonas*. J. Cell Biol. **133:**371–379.
52. **Piperno, G., Z. Ramanis, E. F. Smith, and W. S. Sale.** 1990. Three distinct inner dynein arms in *Chlamydomonas* flagella: molecular composition and location in the axoneme. J. Cell Biol. **110:**379–389.
53. **Pulvermüller, A., A. Gießl, M. Heck, R. Wottrich, A. Schmitt, O. P. Ernst, H.-W. Choe, K. P. Hofmann, and U. Wolfrum.** 2002. Calcium-dependent assembly of centrin–G-protein complex in photoreceptor cells. Mol. Cell. Biol. **22:**2194–2203.
54. **Qin, H., D. R. Diener, S. Geimer, D. G. Cole, and J. L. Rosenbaum.** 2004. Intraflagellar transport (IFT) cargo: IFT transports flagellar precursors to the tip and turnover products to the cell body. J. Cell Biol. **164:**255–266.
55. **Reynolds, E. S.** 1963. The use of lead citrate at high pH as an electron-opaque stain in electron microscopy. J. Cell Biol. **17:**208–212.
56. **Rosenbaum, J. L., and G. B. Witman.** 2002. Intraflagellar transport. Nat. Rev. Mol. Cell Biol. **3:**813–825.
57. **Salisbury, J. L.** 1983. Contractile flagellar roots: the role of calcium. J. Submicrosc. Cytol. **15:**105–110.
58. **Salisbury, J. L.** 1995. Centrin, centrosomes, and mitotic spindle poles. Curr. Opin. Cell Biol. **7:**39–45.
59. **Salisbury, J. L.** 2004. Centrosomes: Sfi1p and centrin unravel a structural riddle. Curr. Biol. **14:**R27–R29.
60. **Salisbury, J. L., A. Baron, B. Surek, and M. Melkonian.** 1984. Striated flagellar roots: isolation and partial characterization of a calcium-modulated contractile organelle. J. Cell Biol. **99:**962–970.
61. **Salisbury, J. L., A. T. Baron, and M. A. Sanders.** 1988. The centrin-based cytoskeleton of *Chlamydomonas reinhardtii*: distribution in interphase and mitotic cells. J. Cell Biol. **107:**635–641.
62. **Salisbury, J. L., K. M. Suino, R. Busby, and M. Springett.** 2002. Centrin-2 is required for centriole duplication in mammalian cells. Curr. Biol. **12:**1287–1292.
63. **Sanders, M. A., and J. L. Salisbury.** 1989. Centrin-mediated microtubule severing during flagellar excision in *Chlamydomonas reinhardtii*. J. Cell Biol. **108:**1751–1760.
64. **Schiebel, E., and M. Bornens.** 1995. In search of a function for centrins. Trends Cell Biol. **5:**197–201.
65. **Schlösser, U. G.** 1994. SAG—Sammlung von Algenkulturen at the University of Göttingen: catalogue of strains. Bot. Acta **107:**113–186.
66. **Scholey, J. M.** 2003. Intraflagellar transport. Annu. Rev. Cell Dev. Biol. **19:**423–443.
67. **Schulze, D., H. Robenek, G. I. McFadden, and M. Melkonian.** 1987. Immunolocalization of a Ca^{2+}-modulated contractile protein in the flagellar apparatus of green algae: the nucleus-basal body connector. Eur. J. Cell Biol. **45:**51–61.
68. **Silflow, C. D., M. LaVoie, L.-W. Tam, S Tousey, M. Sanders, W.-C. Wu, M. Borodovsky, and P. A. Lefebvre.** 2001. The Vfl1 protein in *Chlamydomonas* localizes in a rotationally asymmetric pattern at the distal ends of the basal bodies. J. Cell Biol. **153:**64–74.
69. **Spang, A., I. Courtney, U. Fackler, M. Matzner, and E. Schiebel.** 1993. The calcium-binding protein cell division cycle 31 of *Saccharomyces cerevisiae* is a component of the half-spindle of the spindle pole body. J. Cell Biol. **123:**405–416.
70. **Spang, A., I. Courtney, K. Grein, M. Matzner, and E. Schiebel.** 1995. The cdc31p-binding protein Kar1p is a component of the half bridge of the yeast spindle pole body. J. Cell Biol. **128:**863–878.
71. **Steinkötter, J.** 1997. Centrin und centrinbindende Proteine in Grünalgen. PhD thesis. Botanisches Institut, Universität zu Köln, Cologne, Germany.
72. **Sullivan, D. S., S. Biggins, and M. D. Rose.** 1998. The yeast centrin, Cdc31p, and the interacting protein kinase, Kic1p, are required for cell integrity. J. Cell Biol. **143:**751–765.
73. **Taillon, B. E., S. A. Adler, J. P. Suhan, and J. W. Jarvik.** 1992. Mutational analysis of centrin: an EF-hand protein associated with three distinct contractile fibers in the basal body apparatus of *Chlamydomonas*. J. Cell Biol. **119:**1613–1624.
74. **Tourbez, M., C. Firanescu, A. Yang, L. Unipan, P. Duchambon, Y. Blouquit, and C. T. Craescu.** 2004. Calcium-dependent self-assembly of human centrin 2. J. Biol. Chem. **279:**47672–47680.
75. **Veeraraghavan, S., P. A. Fagan, H. Hu, V. Lee, J. F. Harper, B. Huang, and W. J. Chazin.** 2002. Structural independence of the two EF-hand domains of caltractin. J. Biol. Chem. **277:**28564–28571.
76. **Wiech, H., B. M. Geier, T. Paschke, A. Spang, K. Grein, J. Steinkötter, M. Melkonian, and E. Schiebel.** 1996. Characterization of green alga, yeast, and human centrins. Specific subdomain features determine functional diversity. J. Biol. Chem. **271:**22453–22461.
77. **Wright, R. L., J. Salisbury, and J. W. Jarvik.** 1985. A nucleus-basal body connector in *Chlamydomonas reinhardtii* that may function in basal body localization or segregation. J. Cell Biol. **101:**1903–1912.